nature nanotechnology

LETTERS

PUBLISHED ONLINE: 10 JULY 2011 | DOI: 10.1038/NNANO.2011.100

DNA-based programming of quantum dot valency, self-assembly and luminescence

Grigory Tikhomirov[1†], Sjoerd Hoogland[2†], P. E. Lee[1], Armin Fischer[2], Edward H. Sargent[2*] and Shana O. Kelley[1,3*]

The electronic and optical properties of colloidal quantum dots, including the wavelengths of light that they can absorb and emit, depend on the size of the quantum dots. These properties have been exploited in a number of applications including optical detection[1–3], solar energy harvesting[4,5] and biological research[6,7]. Here, we report the self-assembly of quantum dot complexes using cadmium telluride nanocrystals capped with specific sequences of DNA. Quantum dots with between one and five DNA-based binding sites are synthesized and then used as building blocks to create a variety of rationally designed assemblies, including cross-shaped complexes containing three different types of dots. The structure of the complexes is confirmed with transmission electron microscopy, and photophysical studies are used to quantify energy transfer among the constituent components. Through changes in pH, the conformation of the complexes can also be reversibly switched, turning on and off the transfer of energy between the constituent quantum dots.

To make quantum dot complexes with specific properties it is essential to be able to control the bonding, valency and photophysics of the quantum dots. This means that the quantum dots used to build such complexes must exhibit the following properties, simultaneously (Fig. 1a):

(i) High luminescence efficiency, to enable systematic investigations of quantum dots and their coupled behaviour once assembled into complexes.
(ii) Spectral tunability, to allow control over the direction of energy flow among constituent quantum dots in a single complex. Ideally, the tunability is realized based on systematically varying a single parameter such as quantum dot size achieved with a single-pot synthesis of a single material.
(iii) Control over valency, or rather its analogue in our system, the number of complexation sites available on the surface of a given quantum dot. Selecting the valency would allow control over the number of attachment sites, and therefore the number of nearest neighbours and the dimensionality and architecture of the complexes.
(iv) Control over bonding, including implementing programmable bonding that would permit the precise assembly of different constituents. This ability to control bonding of the building blocks would endow the system with a much greater capacity to build many different types of quantum dot complexes.

DNA was selected as the material that would allow control over these four parameters. DNA – even in the form of short oligonucleotides – offers a high degree of bonding specificity, allowing widely different bond energies to be associated with different quantum dot pairings. Quantum dots are well established as bright luminophores benefiting from wide quantum size-effect tunability in a single materials system[1–7]. DNA-passivated quantum dots are known[8], but have not previously been used to make complex quantum dot assemblies. The challenge was therefore to interface quantum dots with DNA oligonucleotides in a manner that provided control over valency, and to find a single synthetic route for producing brightly emitting quantum dots with spectral tunability which would enable building blocks with variable properties to be prepared from a single material.

Higher-order complexes of nanomaterials have been assembled previously using DNA[8–19]; however, the behaviour of these ensembles differs little from that of the individual components. For example, assemblies of gold nanoparticles have been produced using DNA bonding[11,12,17–19], but these complexes behaved in a manner similar to that of the isolated components. DNA-functionalized quantum dots have also been prepared and assembled, but not with control over valency and the other properties of interest[20–22].

We used a one-pot process that permits the synthesis of bright, stable CdTe nanocrystal quantum dots functionalized with DNA[21] (Fig. 1b). Mercaptopropionic acid (MPA) was used as a co-ligand to passivate sites left open by the DNA. The DNA ligands consisted of three domains (Fig. 1c): a quantum-dot-binding domain featuring phosphorothioate linkages within the backbone; a spacer containing phosphodiester linkages; and a DNA-binding domain also composed of a sequence with phosphodiester linkages. The quantum-dot-binding domain has the highest affinity for the cations of the metal chalcogenide semiconductor quantum dot[23] and thus binds to the surface of the quantum dot, leaving the spacer and DNA-binding domain portion of the sequence unbound. This unbound section of the DNA ligand can then be used for specific binding with a complementary fragment from a different dot. (See Supplementary Information for a description of the assembly process and DNA sequences used.)

The spectral properties of the quantum dots were tuned using specific sequences within the quantum-dot-binding domain. Studies of phosphorothioate oligomers consisting of only five repeating units of A, G, T or C revealed that the highest quantum yields were obtained with G (Fig. 2a). Consistent with earlier observations that G nucleotides serve as the tightest-binding ligands for semiconductor quantum dots[22], we found that oligomers of this base halt the synthesis at an earlier time than those consisting of other bases. This leads to smaller quantum dots (Supplementary Fig. S1) and more stable passivation, which enhances their photoluminescence. Guanine oligomers were therefore used as the

[1]Department of Pharmaceutical Sciences, Leslie Dan Faculty of Pharmacy, University of Toronto, 144 College Street, Toronto, Ontario M5S 3M2, Canada, [2]Department of Electrical and Computer Engineering, University of Toronto, 10 King's College Road, Toronto, Ontario M5S 3G4, Canada, [3]Department of Biochemistry, University of Toronto, 1 King's College Circle, Toronto, Ontario M5S 1A8, Canada; [†]These authors contributed equally to this work. *e-mail: shana.kelley@utoronto.ca; ted.sargent@utoronto.ca

© 2011 Macmillan Publishers Limited. All rights reserved.

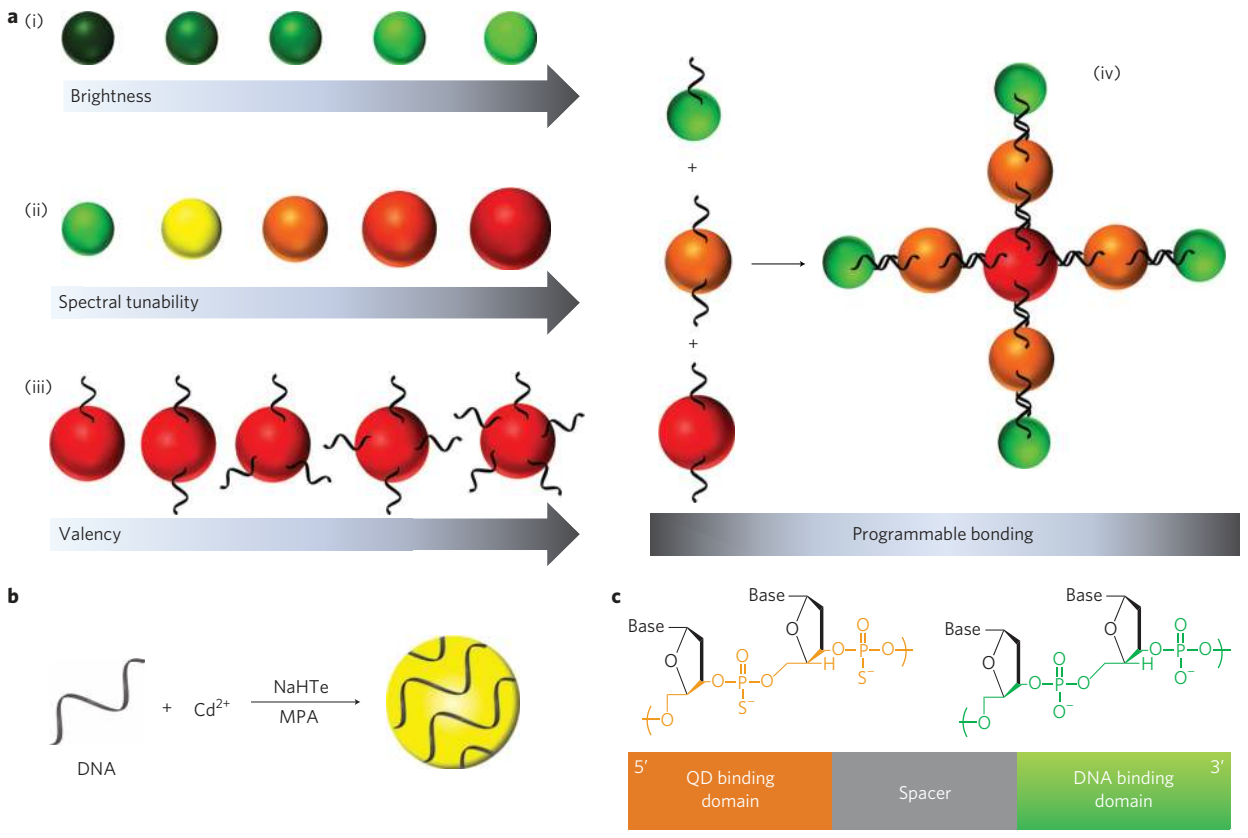

Figure 1 | Synthetic strategy for the development of quantum dots exhibiting strong luminescence, tunable emission spectrum, programmable valency and highly controllable binding energy. a, Schematic depicting control over (i) photoluminescence efficiency, conducive to efficient energy transfer and the realization of highly luminescent quantum dots; (ii) spectral tunability, to generate quantum dots with specific optical properties and allow for efficient energy transfer inside the complexes by matching donor emission and acceptor absorption; (iii) valency, to control the number of binding sites on each quantum dot and therefore to control the assembly of higher-order complexes; and (iv) programmable bonding, to allow selective bonding between specific different quantum dots to generate desired assemblies. **b**, Schematic representation of the synthesis of DNA-capped CdTe quantum dots. **c**, Chemical structure of phosphate and phosphorothioate fragments and the schematic design of DNA strands. QD, quantum dot.

anchoring phosphorothioate sequences to bind the DNA ligand with desired DNA-binding fragments.

The effect of the length of an all-G quantum-dot-binding domain on nanocrystal growth was then studied. As shown in Supplementary Table S1, shorter G oligomers produced smaller quantum dots with higher emission yields and more blueshifted emission relative to longer G oligomers. From this study, it was determined that a range of 5–20 G nucleotides was suitable for the quantum-dot-binding domain. Although G-rich sequences can form quadruplex structures that could interfere with their quantum-dot-binding function, the high temperature at which the reactions are run (100 °C) would denature such structures.

We then investigated the growth of quantum dots as a function of time in the presence of oligonucleotides containing a quantum-dot-binding linker and DNA-binding domain, observing in real time the evolution of the absorption and emission spectra (Fig. 2b). Early in the growth process, the emission maximum was centred at 500 nm, and green-emitting quantum dots could be isolated. After 2 h of growth, the emission maximum was centred around 650 nm, and red-emitting materials could be isolated. Any emission colour between green and red could be chosen by terminating the reaction at an intermediate time. We observed a minor redshift (typically 20 nm) in dot emission wavelength over the course of approximately one day following synthesis (Supplementary Fig. S18).

We used X-ray photoelectron spectroscopy (XPS; Supplementary Section 1.7) to investigate the surface binding and composition of the quantum dots. These measurements confirmed that MPA was bound to the dot surface via the thiol moiety, and indicated the partial replacement of Te by S at the quantum-dot surface. This was previously reported by other groups, and correlated with a similarly high quantum yield of photoluminescence, attributed to improved passivation by a CdS-like shell[24].

In summary, multiple types of quantum-dot building blocks with a variety of energetic properties can be produced from a single reaction. The fact that these nanoparticles emerge from the synthesis with DNA molecules attached and ready to bind to complementary partners is a key element of this approach that differentiates it from other attempts to direct complexation among nanomaterials.

We then turned to the final element of engineering our building blocks: creating polyvalent forms to enable the subsequent assembly of high-order complexes. We were able to synthesize quantum dots with five different valencies (Fig. 2c). This range of valencies was obtained by varying the length of the quantum-dot binding domain. The valencies of quantum dots were evaluated by performing titrations with sequences complementary to the phosphodiester domains displayed on the surfaces of the quantum dots (Supplementary Fig. S4). The binding of sequences to the quantum dots was monitored using size exclusion chromotography. This means of analysis also allowed the binding of non-complementary sequences to be monitored, which were found to be minimal. The inclusion of 20 guanine units in the quantum-dot-binding domain produced quantum dots with one DNA molecule per quantum dot, while 10, 7 and 5 guanine units produced valencies of 2, 3 and 4, respectively. To obtain pentavalent nanoparticles, it was necessary

© 2011 Macmillan Publishers Limited. All rights reserved.

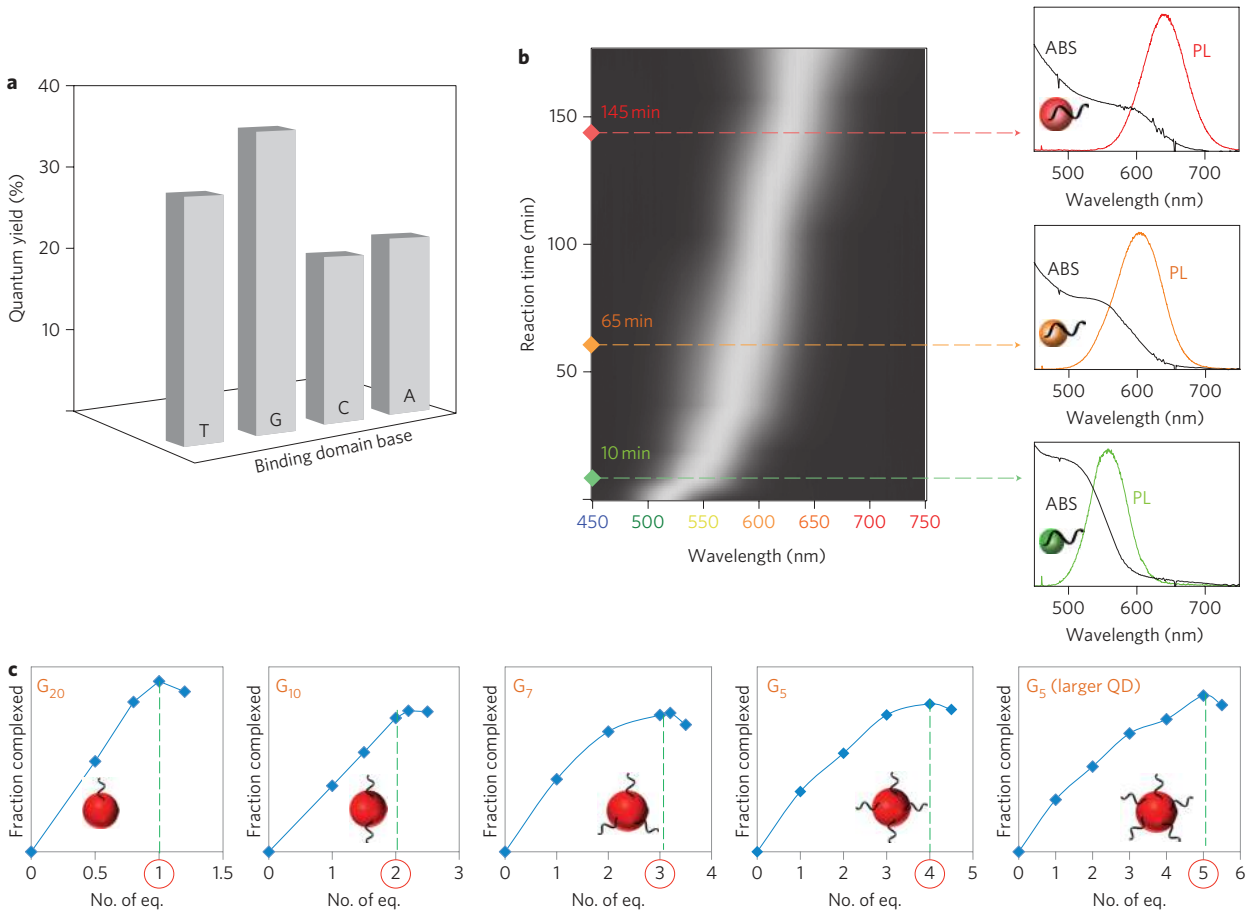

Figure 2 | Experimental results showing control over DNA-programmed quantum dots. a, Luminescence: photoluminescence quantum efficiency of CdTe quantum dots capped with phosphorothioate DNA pentamers containing A, G, T or C residues, showing that dots capped with G-residue pentamers yield the highest luminescence efficiency. The excitation wavelength was 375 nm in all cases. All photoluminescence measurements were carried out on solutions at room temperature. **b**, Quantum dot size/emission wavelength: photoluminescence spectrum as a function of quantum dot synthesis reaction time. After 10, 65 and 145 min of reaction, green-, orange- and red-emitting quantum dots are generated, respectively. Photoluminescence (coloured) and absorption (black) spectra are shown for the three different materials. The sequence used in this trial is G1 (see Supplementary Information for further sequence information). **c**, Valency: size exclusion chromatography results on titration of complementary sequences, showcasing the control over the number of equivalents of complementary DNA which has a direct correlation to the number of available binding sites (see Supplementary Information for sequences and experimental procedures).

to use slightly larger quantum dots to increase the surface area to which the ligands could bind. The desired increase in size was achieved by increasing the reaction time. A typical reaction time for smaller particles (used to generate valencies 1–4) was ~180 min at 100 °C ($\lambda_{max} = 650$ nm). To obtain quantum dots with a valency of 5 ($\lambda_{max} = 680$–690 nm), an additional 50 min of reaction time was necessary (230 min in total). We also found that it was possible to produce quantum dots with asymmetric valency (two different sequences with orthogonal binding properties being displayed on a single quantum dot) if a DNA sequence was used during synthesis that positioned a phosphorothioate sequence between two phosphodiester sequences (Supplementary Fig. S5). The quantum dots produced were stable and resistant to heating (Supplementary Fig. S17); it is noteworthy, however, that some aging was observed following storage of the materials (Supplementary Fig. S18).

We sought to showcase the construction of quantum dot complexes by assembling a variety of different structures based on core quantum dots that were engineered to have different valencies. Figure 3 presents binary complexes comprising 2, 3, 4, 5 or 6 quantum dots, which were successfully assembled using the similar core quantum dot but with different valencies. More intricate structures included linear ternary complexes and cross-shaped ternary complexes, each containing three different types of dots (Fig. 3). Moreover, we were able to program five-member complexes to be branched or linear through selection of the bonding sequences. The precision obtained in the molecular structures can be visualized in the transmission electron microscopy (TEM) images in Fig. 3, in which the different sizes of the constituent quantum dots can be readily observed. Yields of individual complexes typically approached 70%. Complexes were purified after assembly, and high yields of the desired materials in the purified samples were observed by TEM (Supplementary Fig. S3).

We next investigated whether true collective behaviour could be observed that differed from the behaviour of the isolated constituent species. To determine whether the photophysical properties of the quantum dots were altered by their assembly into complexes, we analysed luminescence spectra for a five-membered linear ternary complex (assembled from three different components; Fig. 3, indicated with an asterisk). The smallest-bandgap component, a red quantum dot, was positioned in the centre of the complex so that energy could be funnelled into these acceptors, which would then serve as light emitters. The red quantum dots were constructed to have symmetric divalency so that each would bind two orange dots. The orange dots were engineered to have asymmetric

© 2011 Macmillan Publishers Limited. All rights reserved.

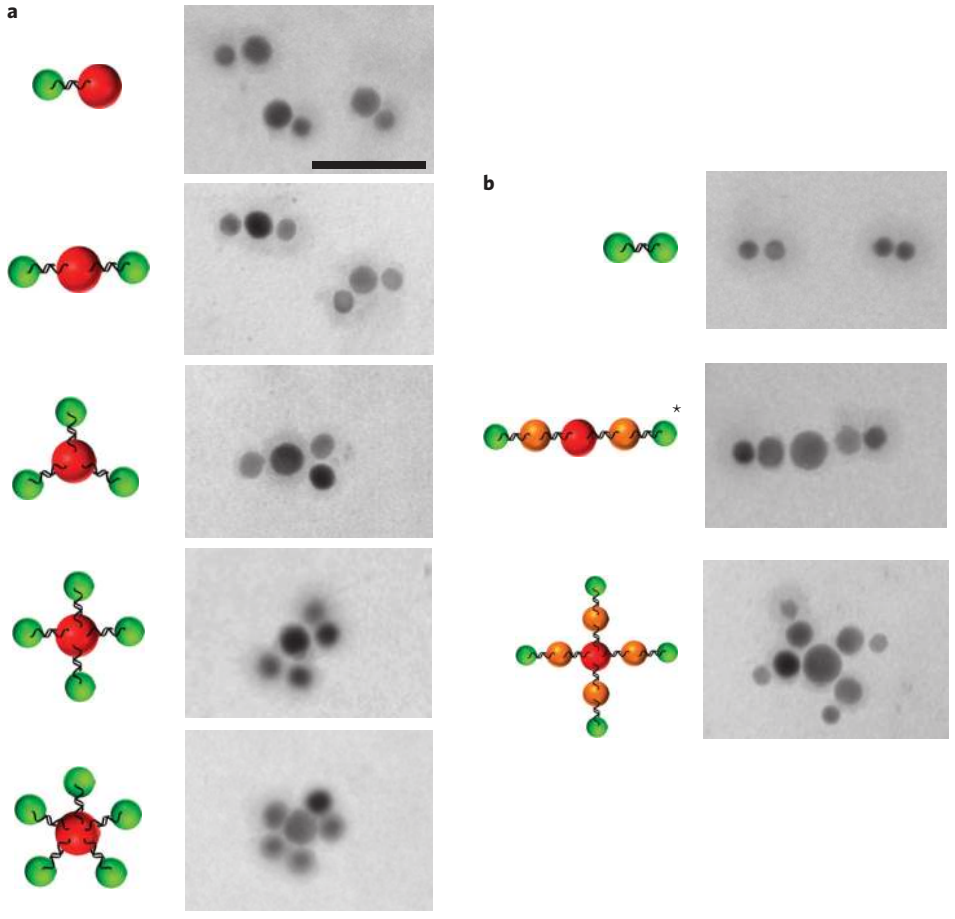

Figure 3 | Representative high-resolution TEM images of DNA-programmed quantum dot complexes. a, Quantum dot assemblies built using red dots with valencies of 1–5 and green dots. **b**, Symmetric binary system made from the same green dots (top); complex structure made from three different dots: linear ternary complex (middle) and cross-shaped ternary complex (bottom). See Supplementary Information for sequences. Scale bar, 10 nm.

divalency so as to bind at one site with the central red dot, with another site left available for specific binding with the green dot (Supplementary Fig. S5). We used monovalent green dots complementary to the second of the two phosphodiester DNA strands on the orange dots. The complex was assembled from a 3:3:1 mixture of the green, orange and red components to ensure full reaction of the red dots. Purification of the complex after assembly by size-selective filtration removed unbound components.

In this complex, the possibility of a cascade of energy from green, via orange, to the red-emitting quantum dot was investigated. As a sensitization (or molecular antenna) strategy, this would offer the potential for a fivefold sensitization gain: at a single excitation wavelength at which the quantum dots have a high optical cross-section, it offers the potential for a fivefold enhancement in red luminescence in our complex over that achieved from a single red emitter.

A comparison of the photoluminescence spectrum of the purified five-component linear ternary complex (Fig. 4b) and the luminescence spectra of the constituent dots (Fig. 4a) clearly indicates that energy transfer occurs within the complex. The luminescence of the three-component assembly is dominated by red-dot emission, with essentially no orange or green emission.

The fraction of light absorbed by each constituent quantum dot within the linear ternary complex was determined by finding the weighting coefficients that allow the absorption spectrum of the complex solution to be expressed as the weighted sum of the absorption spectra of the three constituent dot solutions. As expected, the contribution of the red dots to the complex absorption spectrum was found to be equal to one-fifth, with the orange and green dots each contributing two-fifths (Supplementary Fig. S13). This further (and independently) confirms that the purified five-component linear ternary complex consists of green, orange and red dots in the intended ratio 2:2:1.

We estimated the efficiency of the cascade, as well as uncertainty in this figure-of-merit, by finding the coefficients that would allow the luminescence spectrum of the complex to be described as a superposition of the spectra of the constituent quantum dots (for details see Supplementary Section 2.5). We found that the stepwise energy transfer exceeds 90%. We also carried out time-resolved luminescence studies, finding a significant decrease in the donor excited-state lifetime when it was incorporated into the complex (Supplementary Section 2.10).

Energy transfer between quantum dots of different size, and from polymers to quantum dots, has previously been characterized and found to be efficient[25]. Experimental work has demonstrated that the energy transfer from a polymer to a quantum dot is dependent on the ligand length in a manner consistent with Forster resonance energy transfer (FRET) theory, with ~1 nm ligands leading to 70% efficient energy transfer[25]. In the present work, our short MPA ligands enabled an even higher efficiency to be achieved.

We then investigated the reversibility of the linear ternary assembly. Deoxyribonuclease (DNase) was used to cleave phosphodiester linkages in the DNA backbone, with the goal of deconstructing complexes into their constituent quantum dots. The resultant solution exhibited a luminescence spectrum that closely resembled that of the unhybridized mixture (Fig. 4c). We were able to express the spectrum of the digested complex as a superposition

© 2011 Macmillan Publishers Limited. All rights reserved.

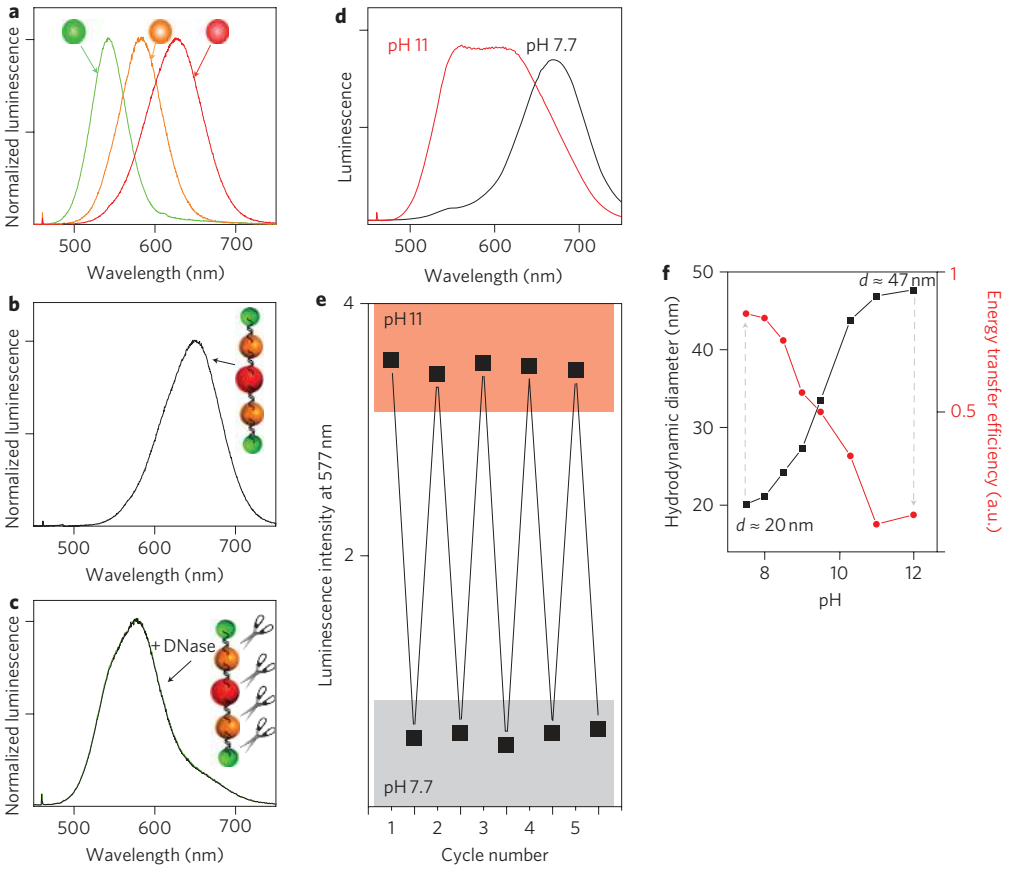

Figure 4 | Optical characteristics of DNA-programmed quantum dot complexes. a–c, Photoluminescence spectra of the constituent green, orange and red quantum dots used as building blocks for higher-order complexes (**a**), the linear ternary complex solution after purification (**b**) (the complex exhibits pure red luminescence and is substantially devoid of the green and orange luminescence that was present before hybridization), and the linear ternary complex after cleavage by DNase, displaying the reversibility of complexation (**c**) (the green curve represents a fit wherein the spectra of the constituents were summed, using weighting coefficients, in an attempt to reproduce the cleaved photoluminescence spectrum). **d**, Photoluminescence spectra at neutral and basic pH. At neutral pH, the complex acts as a coupled entity with all energy transferred to the red dot, whereas at basic pH values, the complex behaves as an ensemble of uncoupled quantum dots. **e**, Photoluminescence intensity at 577 nm as a function of pH cycle number, showing the reversible switching of the complex between the on and off states. **f**, Hydrodynamic diameter (from DLS) and relative energy transfer efficiency (from photoluminescence spectra) as a function of pH for the linear ternary complex solution as measured by DLS. With increasing pH, the complex size increases and the energy transfer efficiency decreases. This change is completely reversible when pH is readjusted to neutral. In all photoluminescence studies, the excitation wavelength was 375 nm.

of the spectra of the constituent quantum dots (Fig. 4c, Supplementary Fig. S15). These observations, combined, prove the reversibility of the process by which we assembled quantum dots into complexes, and further confirm the behaviour of the original assemblies as efficiently coupled complexes.

The pH dependence of the luminescence of the linear ternary assembly was also investigated. Interestingly, energy transfer ceases to occur when the pH is increased above 11 (Fig. 4d), and the luminescence spectrum then resembles the sum of the isolated quantum-dot spectra. The recovery and loss of energy transfer was entirely reversible through many cycles (Fig. 4e), with the onset of energy-transfer decoupling near pH 9 (Supplementary Fig. S21). We evaluated changes in the size of the complex as a function of pH with the aid of dynamic light scattering (DLS) measurements (Fig. 4f). A doubling in the effective hydrodynamic diameter of the complex was observed at high pH, indicating that the complex had assumed an extended conformation under these conditions. With the increase in the hydrodynamic radius, the energy transfer efficiency was reduced. The reversibility of the conformational change, and the pH at which the conformational change occurs, both indicate that disruption of DNA bonding does not occur.

Instead, the ionizable co-ligand used in the DNA–quantum dot synthesis, MPA, may be the source of the behaviour observed. We are able to account for the observation of 'breathing' of the complexes, and, correspondingly, of the turning off of energy transfer when the complexes take on their extended conformation, via the following mechanism. At high pH values, MPA is deprotonated—it takes on the form of mercaptopropionate, the negatively charged conjugate base. Quantum dots passivated using this negatively charged molecule are mutually repelled in the complex, causing it to take on an extended conformation in response to this repulsion. At pH values below the apparent surface pKa of MPA, this molecule is largely uncharged, resulting in less repulsion among the quantum dots making up the complex. The complexes are denser, or less extended in their conformation; as a result, they demonstrate more efficient energy transfer to the lowest-bandgap acceptor. The apparent pKa of MPA has previously been reported to depend strongly on the surface to which the molecule is bound[26]. For example, an apparent pKa lying well above 8 was observed when an MPA self-assembled monolayer was formed on nanostructured noble-metal surfaces. Such an apparent surface pKa is sufficient to explain the transition from a condensed to extended conformation near pH 9 for our assemblies (Fig. 4f). Using gel electrophoresis (Supplementary Fig. S20) as a function of pH, we found that at pH 8 the mobility of the MPA-capped quantum dots was retarded when compared to the mobility at pH 11. This is consistent with

© 2011 Macmillan Publishers Limited. All rights reserved.

MPA-capped dots at pH 11 being considerably more negatively charged than at pH 8.

The modulation of energy transfer efficiency by environment-induced conformational changes is observed frequently in biological systems and particularly in the photosynthetic apparatus that converts light to energy[28–30]. In our complexes, the behaviour arises from a combination of the properties of the DNA 'bonds' that link the nanocrystals, and from the opportunity to tune the donor/acceptor characteristics of, and nearest-neighbour relationships among, the constituent quantum dots.

The findings reported here demonstrate that multi-component, tunable assemblies of quantum dots can be made using DNA as a bonding material. The resultant complexes exhibit versatility and conformation-dependent properties. The set of building blocks described, made using a one-step synthetic method that is accessible to any laboratory that can access synthetic DNA oligonucleotides and a heat block, will be a useful tool set for the construction of nanoscale optoelectronic devices. Moreover, this strategy can be expanded to include other quantum-dot material systems for the construction of even more complex assemblies.

Received 21 February 2011; accepted 31 May 2011; published online 10 July 2011

References

1. Konstantatos, G. *et al*. Ultrasensitive solution-cast quantum dot photodetectors. *Nature* **442,** 180–183 (2006).
2. Clifford, J. P. *et al*. Fast, sensitive and spectrally tuneable colloidal-quantum-dot photodetectors. *Nature Nanotech.* **4,** 40–44 (2009).
3. Konstantatos, G. & Sargent, E. H. Nanostructured materials for photon detection. *Nature Nanotech.* **5,** 391–400 (2010).
4. Sargent, E. H. Infrared photovoltaics made by solution processing. *Nature Photon.* **3,** 325–331 (2009).
5. Huynh, W. U., Dittmer, J. J. & Alivisatos, A. P. Hybrid nanorod–polymer solar cells. *Science* **295,** 2425–2427 (2002).
6. Michalet, X. *et al.* Quantum dots for live cells, *in vivo* imaging, and diagnostics. *Science* **307,** 538–544 (2005).
7. Gao, X., Cui, Y., Levenson, R. M., Chung, L. W. K. & Nie, S. *In vivo* cancer targeting and imaging with semiconductor quantum dots. *Nature Biotechnol.* **22,** 969–976 (2004).
8. Berti, L. & Burley, G. A. Nucleic acid and nucleotide-mediated synthesis of inorganic nanoparticles. *Nature Nanotech.* **3,** 81–87 (2008).
9. Carter, J. D. & Labean, T. H. Organization of inorganic nanomaterials via programmable DNA self-assembly and peptide molecular recognition. *ACS Nano* **5,** 2200–2205 (2011).
10. Ma, N., Sargent, E. H. & Kelley, S. O. Biotemplated nanostructures: directed assembly of electronic and optical materials using nanoscale complementarity. *J. Mater. Chem.* **18,** 954–965 (2008).
11. Nykypanchuk, D., Maye, M. M., van der Lelie, D. & Gang, O. DNA-guided crystallization of colloidal nanoparticles. *Nature* **451,** 549–552 (2008).
12. Alivasatos, A. P. *et al.* Organization of 'nanocrystal molecules' using DNA. *Nature* **382,** 609–611 (1996).
13. Park, S. Y. *et al.* DNA-programmable nanoparticle crystallization. *Nature* **351,** 553–556 (2008).
14. Lee, J. H., Wong, N. Y., Tan, L. H., Wang, Z. & Lu, Y. Controlled alignment of multiple proteins and nanoparticles with nanometer resolution via backbone-modified phosphorothioate DNA and bifunctional linkers. *J. Am. Chem. Soc.* **132,** 8906–8908 (2010).
15. Mitchell, G. P., Mirkin, C. A. & Letsinger, R. L. Programmed assembly of DNA functionalized quantum dots. *J. Am. Chem. Soc.* **121,** 8122–8123 (1999).
16. Ho, Y. P., Kung, M. C., Yang, S. & Wang, T-H. Multiplexed hybridization detection with multicolor colocalization of quantum dot nanoprobes. *Nano Lett.* **5,** 1693–1697 (2005).
17. Zanchet, D., Micheel, C. M., Parak, W. J., Gerion, D. & Alivisatos, A. P. Electrophoretic isolation of discrete Au nanocrystal/DNA conjugates. *Nano Lett.* **1,** 32–35 (2001).
18. Suzuki, K., Hosokawa, K. & Maeda, M. Controlling the number and positions of oligonucleotides on gold nanoparticle surfaces. *J. Am. Chem. Soc.* **131,** 7518–7519 (2009).
19. Zhao, W. T. & Hsing, I. M. Facile and rapid manipulation of DNA surface density on gold nanoparticles using mononucleotide-mediated conjugation. *Chem. Commun.* **46,** 1314–1316 (2010).
20. Ma, N., Yang, J., Stewart, K. M. & Kelley, S. O. DNA-passivated CdS nanocrystals: luminescence, bioimaging, and toxicity profiles. *Langmuir* **23,** 12783–12787 (2007).
21. Ma, N., Sargent, E. H. & Kelley, S. O. One-step DNA-programmed growth of luminescent and biofunctionalized nanocrystals. *Nature Nanotech.* **4,** 121–125 (2009).
22. Hinds, S. *et al.* Nucleotide-directed growth of semiconductor nanocrystals. *J. Am. Chem. Soc.* **128,** 64–65 (2006).
23. Pecoraro, V. L., Hermes, J. D. & Cleland, W. W. Stability constants of Mg^{2+} and Cd^{2+} complexes of adenine nucleotides and thionucleotides and rate constants for formation and dissociation of MgATP and MgADP. *Biochemistry* **23,** 5262–5271 (1984).
24. Borchert, H. *et al*, Relations between the photoluminescence efficiency of CdTe nanocrystals and their surface properties revealed by synchrotron XPS. *J. Phys. Chem. B* **107,** 9662–9668 (2003).
25. Chang, T-W. F. *et al.* Efficient excitation transfer from polymer to nanocrystals. *Appl. Phys. Lett.* **84,** 4295–4297 (2004).
26. Burris, S. C., Zhou, Y., Maupin, W. A., Ebelhar, A. J. & Daugherty, M. W. The effect of surface preparation on apparent surface pKas of mercaptocarboxylic acid self-assembled monolayers on polycrystalline gold. *J. Phys. Chem. C* **112,** 6811–6815 (2008).
27. Fu, A. *et al.* Discrete nanostructures of quantum dots/Au with DNA, *J. Am. Chem. Soc.* **126,** 10832–10833 (2004).
28. Wilk, K. E. *et al.* Evolution of a light-harvesting protein by addition of new subunits and rearrangement of conserved elements: crystal structure of a cryptophyte phycoerythrin at 1.63 Å resolution. *Proc. Natl Acad. Sci. USA* **96,** 8901–8906 (1999).
29. Wohri, A. B. *et al* Light-induced structural changes in a photosynthetic reaction center caught by Laue diffraction. *Science* **328,** 630–633 (2010).
30. Pascal, A. A. *et al.* Molecular basis of photoprotection and control of photosynthetic light-harvesting. *Nature* **436,** 134–137 (2005).

Acknowledgements

The authors acknowledge support from the National Institutes of Health (R21 to S.O.K.), the Ontario Research Fund (ORF-RE to S.O.K. and E.H.S.) and the Canada Research Chairs programme (E.H.S.).

Author contributions

G.T. and S.O.K. designed the protocols for the synthesis of the nanoparticles and complexes. S.H., G.T. and E.H.S. designed and interpreted the energy transfer studies. G.T., P.E.L. and A.F. carried out materials analysis, and worked with E.H.S. and S.O.K. in their interpretation. E.H.S. and S.O.K. co-wrote the paper with contributions from G.T., S.H., A.F. and P.E.L.

Additional information

The authors declare no competing financial interests. Supplementary information accompanies this paper at www.nature.com/naturenanotechnology. Reprints and permission information is available online at http://www.nature.com/reprints/. Correspondence and requests for materials should be addressed to E.H.S. and S.O.K.

© 2011 Macmillan Publishers Limited. All rights reserved.